

## CD163+ M2 macrophages promote fibrosis in IgG4-related disease via TLR7/IRAK4/NF- $\kappa$ B signaling

鎮守, 晃

<https://hdl.handle.net/2324/4795544>

---

出版情報 : 九州大学, 2022, 博士 (歯学), 課程博士  
バージョン :  
権利関係 :



**CD163<sup>+</sup> M2 macrophages promote fibrosis in IgG4-related disease via  
TLR7/IRAK4/NF- $\kappa$ B signaling**

**Running head: M2 macrophage-induced fibrosis in IgG4-related disease**

Akira Chinju, DDS<sup>1</sup>, Masafumi Moriyama, DDS, PhD<sup>1,2</sup>, Noriko Kakizoe-Ishiguro, DDS, PhD<sup>1</sup>, Hu Chen, DDS<sup>1</sup>, Yuka Miyahara, DDS<sup>1</sup>, A.S.M. Rafiul Haque, DDS, PhD<sup>3</sup>, Katsuhiro Furusho DDS, PhD<sup>4</sup>, Mizuki Sakamoto, DDS<sup>1</sup>, Kazuki Kai, DDS<sup>1</sup>, Kotonno Kibe, DDS<sup>1,5</sup>, Sachiko Hatakeyama-Furukawa DDS, PhD<sup>1</sup>, Miho Ito-Ohta, DDS, PhD<sup>1</sup>, Takashi Maehara, DDS, PhD<sup>1</sup>, and Seiji Nakamura, DDS, PhD<sup>1</sup>

<sup>1</sup>Section of Oral and Maxillofacial Oncology, Division of Maxillofacial Diagnostic and Surgical Sciences, Faculty of Dental Science, Kyushu University, Fukuoka, Japan

<sup>2</sup>OBT Research Center, Faculty of Dental Science, Kyushu University, Fukuoka, Japan

<sup>3</sup>Department of Dental Anatomy, Udayan Dental College, Rajpara, Bangladesh.

<sup>4</sup>Sleep and Aging Regulation Research Project Team, National Center for Geriatrics and Gerontology, Aichi, Japan

<sup>5</sup>Division of Innate Immunity, Department of Microbiology and Immunology, Institute of Medical Science, University of Tokyo, Tokyo, Japan

**Corresponding author:** Masafumi Moriyama

Section of Oral and Maxillofacial Oncology, Division of Maxillofacial Diagnostic and Surgical Sciences, Faculty of Dental Science, Kyushu University, 3-1-1 Maidashi, Higashi-ku, Fukuoka 812-8582, Japan.

This article has been accepted for publication and undergone full peer review but has not been through the copyediting, typesetting, pagination and proofreading process which may lead to differences between this version and the [Version of Record](#). Please cite this article as doi: [10.1002/art.42043](https://doi.org/10.1002/art.42043)

Tel: +81-92-642-6447; Fax: +81-92-642-6386; E-mail: moriyama@dent.kyushu-u.ac.jp

**Financial Support:** This study was supported by the Ministry of Education, Culture, Sports, Science, and Technology of Japan (Grant Numbers: 21H03141, 20H00553) and the MHLW Research Program on Rare and Intractable Diseases (Grant Number: JPMH20FC1040).

**Conflict of Interest:** The authors declare that they have no conflict of interest.

## Abstract

**Objective:** IgG4-related disease (IgG4-RD) is a fibro-inflammatory condition that can affect multiple organs. We previously demonstrated that human Toll-like receptor 7 (*huTLR7*)-transgenic C57BL/6 mice showed elevated serum IgG1 levels and inflammation with fibrosis in the salivary glands (SGs), lungs, and pancreas. Moreover, we observed extensive TLR7<sup>+</sup>CD163<sup>+</sup> M2 macrophage infiltration in SGs from IgG4-RD patients. Here, we examined the fibrotic mechanism via the TLR7 pathway.

**Methods:** Gene expression in SGs from *huTLR7*-transgenic mice and IgG4-RD patients was analyzed using DNA microarrays. We extracted the common upregulated TLR7-related genes in SGs from *huTLR7*-transgenic mice and IgG4-RD patients. Finally, we investigated the interaction between CD163<sup>+</sup> M2 macrophages and fibroblasts before/after stimulation with the TLR7 agonist loxoribine.

**Results:** In *huTLR7*-transgenic mice and IgG4-RD patients, IL-1 receptor-associated kinase 3 (IRAK3) and IRAK4 were significantly overexpressed. Real-time PCR validated the upregulation of only IRAK4 in IgG4-RD patients compared with the other groups. IRAK4 was strongly detected in/around germinal centers in SGs from IgG4-RD patients alone. Double immunofluorescence staining showed that IRAK4-positive cells were mainly co-localized with CD163<sup>+</sup> M2 macrophages in SGs. After stimulation with loxoribine, CD163<sup>+</sup> M2 macrophages exhibited significantly enhanced expression of IRAK4 and nuclear factor kappa B (NF-κB) and increased supernatant concentrations of fibrotic cytokines. Finally, we confirmed that the number of fibroblasts was increased by culture with the supernatant of CD163<sup>+</sup> M2 macrophages following stimulation with loxoribine.

**Conclusion:** CD163<sup>+</sup> M2 macrophages promote fibrosis in IgG4-RD by increasing the production of fibrotic cytokines via TLR7/IRAK4/NF-κB signaling.

**Keywords:** IgG4-related disease, M2 macrophage, Toll-like receptor 7, IL-1 receptor-associated kinase 4, fibrosis

## Introduction

IgG4-related disease (IgG4-RD) is an immune-mediated systemic condition affecting various organs including the lacrimal glands, submandibular glands (SMGs), kidneys, lungs, thyroid, liver, bile ducts, pancreas, prostate, aorta, lymph nodes, and mammary glands (1-3). Increased serum IgG4 levels and sclerosing changes with abundant IgG4-positive plasma cells and severe fibrosis are the main clinical features of IgG4-RD (4).

Although the pathogenic involvement of adaptive immune responses mediated by T helper (Th) cells and plasmablasts in IgG4-RD is well established (5-12), recent studies highlighted the innate immune responses underlying the immunopathogenesis of IgG4-RD (13-15). We previously confirmed the extensive infiltration of M2 macrophages expressing CD163 in salivary glands (SGs) from patients with IgG4-RD, which indicates that M2 macrophages contribute to tissue fibrosis via the production of pro-fibrogenic factors including CC motif chemokine ligand 18 (CCL18) and interleukin-10 (IL-10) (16), as well as the activation of T helper type 2 immune responses via IL-33 secretion (17). Moreover, recent studies indicated that Toll-like receptors (TLRs), which are important for innate immunity, are associated with the pathogenesis of IgG4-RD (18-20). Fukui et al (21) examined the number of TLR1-TLR11 positive cells in pancreatic tissues from IgG4-related autoimmune pancreatitis (AIP) patients.

The ratio of TLR7-positive to infiltrated monocytes/macrophages was significantly higher in type 1 AIP patients. We also reported the accumulation of TLR7<sup>+</sup>CD163<sup>+</sup> M2 macrophages in SMGs from patients with IgG4-RD (17). Interestingly, our recent data confirmed that human *TLR7*-transgenic/*mTlr7* deficient (*huTLR7*-transgenic/*mTlr7*<sup>-/-</sup>) mice exhibited a phenotype similar to that of IgG4-RD patients. Specifically, fibro-inflammation in the SMGs, pancreas, and lungs was shown in *huTLR7*-transgenic/*mTlr7*<sup>-/-</sup> mice compared with wild-type mice. In addition, the serum concentrations of IgG, IgG1 (equivalent to human IgG4), and IL-33 in *huTLR7*-transgenic/*mTlr7*<sup>-/-</sup> mice were markedly increased following stimulation with a TLR7 agonist. This indicated that TLR7 signaling is associated with the pathogenesis of IgG4-RD (22). However, it remains unknown why *huTLR7*-transgenic/*mTlr7*<sup>-/-</sup> mice exhibit a phenotype similar to IgG4-RD patients. Here, we investigated the downstream events of TLR7 signaling in *huTLR7*-transgenic/*mTlr7*<sup>-/-</sup> mice and IgG4-RD patients to clarify the fibrotic mechanism that contributes to IgG4-RD.

## **Patients and Methods**

### ***Study participants***

The study protocol was approved by the accredited Medical Ethical Committees of Kyushu University Hospital (approval nos. 25-287 and 26-86). All patients provided written informed consent prior to participation. The study was conducted in accordance with the ethical principles of the Declaration of Helsinki, and the approved guidelines of Kyushu University Hospital.

Peripheral blood and SGs were obtained from patients with IgG4-RD (n = 15), primary Sjögren's syndrome (pSS) (n = 15), or chronic sialadenitis (CS) (n = 15), as well as healthy controls (HCs) (n = 15) recruited from the Department of Oral and Maxillofacial Surgery, Kyushu University Hospital between 2012 and 2020. Details of the clinical profiles of the IgG4-RD patients are available in online Supplementary Table 1. Healthy donors were defined by a lack of any current history or history of malignancy, autoimmune disease, or chronic infections.

We performed labial salivary gland biopsy and open SMG incisional biopsy in IgG4-RD and pSS patients as previously described (23), and SG extraction in CS patients. IgG4-RD was diagnosed with reference to “The 2020 revised comprehensive diagnostic criteria for IgG4-related disease” (24) and “Diagnostic criteria for IgG4-DS” (25). All patients with IgG4-RD showed typical histopathological findings, including marked



Accepted Article

infiltration of IgG4-positive plasma cells, severe fibrosis, and formation of multiple ectopic germinal centers (eGCs), and had not received previous treatment with steroids or other immunosuppressants. SS was diagnosed according to the Research Committee on SS of the Ministry of Health, Labour and Welfare of the Japanese Government (1999) (26) and the American College of Rheumatology/European League Against Rheumatism Classification Criteria for pSS (2016) (27).

All patients with SS exhibited lymphocytic infiltration in SGs, had no other autoimmune diseases, and had not received previous treatment with steroids or other immunosuppressants. There was no documented history of human immunodeficiency virus, human T-cell lymphotropic virus type 1, hepatitis B virus, or hepatitis C virus infection in any of the patients. None of the patients had evidence of malignant lymphoma at the time of the study. As a comparative healthy sample, salivary glands, tonsils, and lymph nodes were obtained from patients with oral squamous cell carcinoma (OSCC) at tumor resection. These samples from OSCC patients were histologically normal and lacked clinical evidence of metastasis or radiation therapy, and were defined as healthy controls (HCs).

#### ***Gene expression microarrays***

Accepted Article

In accordance with the manufacturer's instructions, complementary RNA was amplified and labeled using the Low Input Quick Amp Labeling Kit (Agilent Technologies, Santa Clara, CA, USA) and hybridized to SurePrint G3 Human Gene Expression Microarrays 8 60K v2 (Agilent Technologies) (DNA chip including 60,000 genes). All hybridized microarray slides were scanned using an Agilent scanner. Relative hybridization intensities and background hybridization values were calculated using Agilent Feature Extraction Software (ver. 9.5.1.1) as previously described (28).

#### ***Real-time quantitative PCR***

Total RNA was isolated from SGs using an RNeasy RNA extraction kit (Qiagen, Hilden, Germany), and complementary DNA (cDNA) was synthesized as previously described (29). The resulting cDNA was amplified using the PowerUp™ SYBR Green Master Mix (Thermo Fisher Scientific Inc., Waltham, MA, USA) in an AriaMx Real-Time PCR instrument (version 1.7; Agilent Technologies). The levels of mRNA for *TLR7*, IL-1 receptor-associated kinase 3 (*IRAK3*), *IRAK4*, *MyD88*, interferon regulatory factor 5 (*IRF5*), *IRF7*, tumor necrosis factor receptor-associated factor 6 (*TRAF6*), nuclear factor kappa B (*NFκB*), actin alpha 2 (*ACTA2*), and fibroblast activation protein (*FAP*) were analyzed. The relative mRNA levels were calculated after normalizing to the housekeeping gene β-actin.

The primer sequences used are described in the online Supplementary Method 1. All analyses were performed in triplicate.

### ***Immunohistochemical analysis***

The SG samples were cut to 4- $\mu$ m-thick formalin-fixed and paraffin-embedded sections, and immunohistochemical staining was performed for CD11c, CD80, CD123, CD163, IRAK3, and IRAK4 as previously described (23). Details of the antibodies used in this study are shown in Supplementary Table 2. Hematoxylin counterstaining was performed after immunohistochemical staining. For multi-immunofluorescence analyses, the 4- $\mu$ m-thick histological sections of SGs were stained with anti-CD163, anti-CD123, anti-CD11c, anti-IRAK4, and anti-CD80 antibodies using an Opal 4-Color Manual IHC Kit (catalog no. #NEL810001KT; PerkinElmer), and analyzed under a light microscope (IX83, Olympus Corporation, Tokyo, Japan).

### ***Quantitative image analysis***

TissueQuest software (TissueGnostics, Los Angeles, CA, USA) provides automated high-resolution imaging with the scientific accuracy of flow cytometry

(<http://www.bga.su/info/TissueFAXS>). Stained cells were automatically counted in the SG

specimens. Staining of SG specimens was quantified using TissueQuest software, with cut-off values determined relative to the positive controls as previously described (7).

### ***Evaluation of the severity of fibrosis***

Masson's trichrome (MT) staining utilizes three stains to selectively identify fibrotic areas (blue), nuclei (dark brown), and cytoplasm (red). The fibrosis score is calculated from the ratio of the fibrotic area (blue) to the whole stained area in a 4- $\mu\text{m}^2$  field of view, from 5 different areas.

### ***In vitro experiments***

CD163<sup>+</sup> M2 macrophages were isolated from healthy peripheral blood mononuclear cells as described in a previous report (22), and were then stimulated with 500  $\mu\text{M}$  of the TLR7 agonist loxoribine (catalog no. #ALX-480-097-M025; Enzo Life Sciences, Farmingdale, NY, USA) and/or 1  $\mu\text{M}$  of the IRAK4 inhibitor CA-4948 (catalog no. #CA-4948; Selleck, Houston, TX, USA) (online Supplementary Figures 1 and 2). The supernatants and RNA were collected for further analysis.

### ***In vivo experiments***

To examine the *in vivo* function of human TLR7 (huTLR7), we established *mTlr7* deficient mice and *huTLR7*-transgenic/*mTlr7*<sup>-/-</sup> (Tg) mice on a C57BL/6 background as described in a

previous report (22). For the TLR7 ligand treatment of Tg mice, their ear skin was topically treated 3 times a week with 100 µg of resiquimod (R848; ChemScene Chemicals, Monmouth Junction, NJ, USA) in 100 µl of acetone.

### ***Statistical analysis***

Data are presented as the mean ± SD. Student's *t*-test, Mann–Whitney *U*-test,  $\chi^2$  test, Kruskal–Wallis tests, and Spearman's rank correlations were used to calculate the statistical significance of differences between groups. A *P*-value of < 0.05 was considered statistically significant. All analyses were performed using GraphPad Prism 9 (GraphPad Software, San Diego, CA, USA).

### ***Additional detail.***

Reagents and more detailed methods for the isolation of CD163<sup>+</sup> M2 macrophages, establishment of Tg mice, flow cytometry analysis, ELISA, cell proliferation assay, and cell division assay are described in the Supplementary Methods and online Supplementary Figures 1 and 2.

## **Results**

### ***Phenotype of huTLR7-transgenic/*mTlr7*<sup>-/-</sup> mice***

Accepted Article

As mentioned above, we established *huTLR7-transgenic/mTlr7<sup>-/-</sup>* (Tg) mice as a model of IgG4-RD. To confirm the phenotype of Tg mice, 4-week-old Tg and *mTlr7<sup>-/-</sup>* (KO) mice were stimulated with a TLR7 agonist (R848) for 4 weeks (Figure 1A). Histological and serological examinations were performed with Tg and KO mice treated with the TLR7 agonist. Representative histological findings in the SMGs from Tg and KO mice are shown in Figure 1B. The degree of lymphocytic infiltration in the SMGs from Tg mice was markedly increased compared with that in the SMGs from KO mice. Moreover, we evaluated the degree of fibrosis in SMGs specimens by MT staining. The fibrosis scores in the SMGs from Tg mice were significantly higher than those in the SMGs from KO mice (Figure 1C). Furthermore, Tg mice had significantly high levels of serum IgG and IgG1 after TLR7 agonist stimulation compared with KO mice (Figure 1D). Murine IgG1 is considered to be functionally equivalent to human IgG4.

#### ***Gene expression profiles of TLR7- and fibrosis-related genes in SMGs from Tg mice***

Gene expression profiling by DNA microarray was performed to evaluate the differences in gene expression of SMG samples between Tg and KO mice. The heat map for TLR7- and fibrosis-related genes is shown in Figure 1E. The expression levels of the TLR7-related genes, *Irf5*, *Irak3*, and *Irak4* were significantly increased in Tg mice compared with KO mice. In

Accepted Article

addition, Figure 1F shows a heat map for the differences in TLR7- and fibrosis-related gene expression levels between IgG4-RD patients and HCs. The expression levels of the TLR7-related genes *IRF3*, *IRF5*, *IRF7*, *TRAF6*, *IRAK3*, *IRAK4*, and *MyD88* were significantly higher in IgG4-RD patients compared with HCs. Thus, we focused on *IRF5*, *Irak3*, and *Irak4*, which are commonly upregulated TLR7-related genes in Tg mice and IgG4-RD patients. The validation of the real-time PCR for the detection of these common candidate TLR7-related genes was subsequently performed by increasing the number of cases.

#### ***Validation of candidate TLR7-related genes in SGs***

As shown in Figure 1G, the mRNA expression levels of *Irak4* were significantly higher in SMGs from Tg mice compared with those in KO mice. Furthermore, the mRNA expression levels of *IRAK4* were significantly higher in SGs from patients with IgG4-RD compared with those from the other groups, including patients with CS or SS and HCs (Figure 1H). The SG specimens were examined by immunohistochemistry to confirm the expression and distribution of candidate TLR7-related molecules, including *IRF5*, *IRAK3*, and *IRAK4* (online Supplementary Figure 3). Representative findings of *IRAK4* are shown in Figure 2A and B. Based on morphological identification, *IRAK4* expression was detected in infiltrating inflammatory cells in the tissues from Tg mice but not KO mice (Figure 2A). In addition, the

Accepted Article

samples of patients from patients with IgG4-RD showed the enhanced infiltration of IRAK4-positive cells around eGCs compared with those from patients with CS or SS and HCs (Figure 2B).

Because these control disease components are quite different from IgG4-RD, we examined the secondary lymphoid tissues of HCs. IRAK4 was detected at low levels around eGCs in the tonsils of HCs but frequently detected around the eGCs in SMGs from patients with IgG4-RD (Figure 2C). Moreover, the number of IRAK4<sup>+</sup> cells was significantly higher in IgG4-RD than in the other groups (Figure 2D).

#### ***Identification of IRAK4-expressing cells in SMGs***

Because IRAK4 is mainly expressed in macrophages and dendritic cells (DCs) (25), SMG specimens from patients with IgG4-RD were stained for CD80 (marker for M1 macrophages), CD163 (M2 macrophages), CD11c (myeloid DCs), CD123 (plasmacytoid DCs), and IRAK4. The strong expressions of CD163-, CD11c-, and IRAK4-positive cells were observed in fibrotic areas and around eGCs, whereas the minimal expressions of CD80- and CD123-positive cells were observed around the eGCs (Figure 2E).

To identify the IRAK4-expressing cells in inflamed IgG4-RD tissues, SMG specimens from patients with IgG4-RD were stained with immunofluorescent antibodies to IRAK4 (red), CD80



(green), CD163 (green), CD11c (green), CD123 (green), and DAPI (blue). We observed that many CD163-positive cells were co-localized with IRAK4 in IgG4-RD tissues (Figure 2F).

Furthermore, we performed quantitative analysis of the distributions of IRAK4-expressing CD80-, CD163-, CD11c-, or CD123-positive cells in IgG4-RD tissues and found a significantly higher number of IRAK4-expressing CD163-positive cells compared with other evaluated cells (Figure 2G).

#### ***Inflammatory cytokine production in M2 macrophages via TLR7/IRAK4 signaling***

We examined the effect of a TLR7 agonist (loxoribine) and IRAK4 inhibitor (CA-4948) on CD163<sup>+</sup> M2 macrophages *in vitro* (Figure 3A). First, we confirmed the expression of TLR7 in CD163<sup>+</sup> M2 macrophages after differentiation and extraction, as described in the Patients and Methods section. The downstream pathways of TLR7 are shown in Figure 3C. *MyD88*, *IRAK4*, *TRAF6*, and *NF-κB* exhibited increased expression following treatment with the TLR7 agonist, whereas *IRAK4*, *TRAF6*, and *NF-κB* were downregulated by the IRAK4 inhibitor (Figure 3D). Next, we determined the concentration of fibrotic cytokines (IL-33, IL-1β, and TGF-β) in culture supernatants with/without the TLR7 agonist and IRAK4 inhibitor. The concentrations of IL-33, IL-1β, and TGF-β in the culture supernatant were significantly increased after stimulation with the TLR7 agonist. Furthermore, the concentrations of these cytokines were

significantly decreased in the presence of the IRAK4 inhibitor (Figure 3E).

***Effect of the TLR7 agonist and IRAK4 inhibitor on the proliferation and activation of fibroblasts***

Because our recent data indicated that M2 macrophages might promote fibrosis in the local lesions from patients with IgG4-RD (13), we evaluated the *in vitro* response of fibroblasts (MRC-5 cells) to culturing in the conditional medium (CM) derived from CD163<sup>+</sup> cells treated with the TLR7 agonist and/or IRAK4 inhibitor (Figure 4A). On day 4, a higher cell density was observed for fibroblasts cultured in the CM derived from CD163<sup>+</sup> cells treated with the TLR7 agonist compared with the CM alone or the CM treated with the TLR7 agonist and IRAK4 inhibitor (Figure 4B). Next, we performed a cell proliferation assay, which indicated that cell viability in MRC-5 cells cultured in the CM derived from CD163<sup>+</sup> cells treated with the TLR7 agonist was significantly greater than that in the other CMs (Figure 4C). Additionally, a cell division assay revealed an increased cell division rate of MRC-5 cells cultured in the CM derived from CD163<sup>+</sup> cells treated with the TLR7 agonist compared with that in the other CMs (online Supplementary Figure 4). Moreover, increased ACTA2 and FAP expressions and higher type 1 collagen levels were detected in these cells (Figure 4D, E).

***Evaluation of fibrosis scores in SMGs***

Accepted Article

Finally, we investigated the relationships between fibrosis scores and the number of IRAK4- or CD163-positive cells in SMGs from patients with IgG4-RD. Specimens were stained with MT to evaluate the degree of fibrosis in the SMGs. The fibrosis scores determined by MT staining were defined as described in the Patients and Methods section. The tissues from IgG4-DS patients showed severe cordlike fibrosis and extensive eGC formation (Figure 5A). The fibrosis score was positively correlated with the number of IRAK4<sup>+</sup> and CD163<sup>+</sup> cells (Figure 5B).

## Discussion

IgG4-RD is pathologically characterized by the dense infiltration of lymphocytes/plasma cells, obliterative phlebitis, and marked fibrosis (termed “storiform fibrosis”) (31). In particular, marked fibrosis often irreversibly impairs the functions of affected organs, such as the pancreas, kidneys, and lungs, in patients with diabetes, renal insufficiency, and interstitial pneumonia, respectively. Therefore, the elucidation of the fibrotic mechanism in IgG4-RD is essential for the prevention of organ dysfunction.

Recently, several studies demonstrated that innate immune cells such as basophils, pDCs, and M2 macrophages might be involved in the initiation and fibrosis of IgG4-RD (18-20) or

the phenotypes of other mouse models (32,33) via TLR signaling. The dominant infiltration of basophils expressing TLR2 and/or TLR4 was shown in the pancreatic lesions of IgG4-related AIP (18). Notably, Watanabe et al. (34) suggested that IFN- $\alpha$  and IL-33 produced by pDCs promoted chronic fibro-inflammatory responses underlying the AIP model mouse and human IgG4-related AIP.

M2 macrophages (alternatively known as activated macrophages) are induced by IL-4 and are known to have a critical role in tissue repair and the progression of fibrotic diseases (35,36). Previously, we examined the involvement of M2 macrophages in the fibrosis of SMGs from patients with IgG4-RD, SS, and CS and indicated that the fibrosis score was positively correlated with the frequency of M2 macrophages in SMGs from IgG4-DS patients but not in those from the other groups (16). These results suggest that M2 macrophages might preferentially promote the fibrosis of affected lesions in IgG4-RD patients. In addition, our recent data demonstrated that TLR7-expressing M2 macrophages may contribute to the fibrotic inflammation of affected organs via IL-33 secretion in IgG4-RD patients and *huTLR7*-transgenic mice (22), but the details of the fibrosis mechanism in IgG4-RD via the downstream pathways of TLR7 signaling remain unknown. TLR7, mainly expressed on macrophages and DCs, recognizes several synthetic compounds and ssRNAs of viruses.

Accepted Article

Ewald et al. (37) suggested that TLR7 recognizes exogenous and endogenous RNAs from damaged tissues or apoptotic cells and can contribute to the pathogenesis of autoimmune and allergic diseases. In this study, we performed differential expression analysis using DNA microarrays to investigate TLR7-related molecules in the SMGs of *huTLR7*-transgenic mice and IgG4-RD patients.

Microarray analysis of SMGs demonstrated significant increases in the TLR-7-related genes *IRF5*, *IRAK3*, and *IRAK4* in *huTLR7*-transgenic mice and IgG4-RD patients. In addition, validation by quantitative real-time PCR and immunohistochemical staining revealed the overexpression of IRAK4 in SMGs from patients with IgG4-RD compared with the other groups. IRAK4 is a critical component of the TLR/IL-1 receptor signaling pathway and has an important role in the innate immune system and inflammation (38,39). Moreover, Leah et al. (40) demonstrated that the inhibition of IRAK4 decreased the production of several inflammatory cytokines (IL-1 $\beta$ , IL-6, and tumor necrosis factor- $\alpha$ ) in TLR7 agonist (R848)-treated human monocytes via the activation of NF- $\kappa$ B. We confirmed that TLR7<sup>+</sup>CD163<sup>+</sup> M2 macrophages secreted IL-33, IL-1 $\beta$ , and TGF- $\beta$  via TLR7/IRAK4/NF- $\kappa$ B signaling pathways, which promoted the activation and proliferation of human fibroblasts *in vitro* (Figure 4). In addition, the fibrosis scores were positively correlated with the number of

CD163<sup>+</sup> and IRAK4<sup>+</sup> cells in patients with IgG4-DS (Figure 5). The results presented here confirm that CD163<sup>+</sup> M2 macrophages promote the fibrosis of swollen lesions from IgG4-RD patients via IRAK4 signaling. Moreover, we previously reported the abundant infiltration of IL-1 $\beta$ - and TGF- $\beta$ 1-secreting CD4<sup>+</sup> cytotoxic T lymphocytes (CTLs) in the peripheral blood and inflammatory tissue lesions of IgG4-RD patients (7). These active cytokine-secreting effector CD4<sup>+</sup> CTLs are linked to chronic inflammation and fibrosis.

In conclusion, based on our data reported here and published previously, a proposed model for the fibrotic mechanism in IgG4-RD is shown in Figure 6. TLR7-expressing M2 macrophages in affected organs recognize some viral RNAs or self RNAs released from stressed or injured cells and promote the production of several fibrotic cytokines (IL-33, IL-1 $\beta$ , and TGF- $\beta$ ) via TLR7/IRAK4/NF- $\kappa$ B signaling, which leads to severe fibrosis in affected organs. Thus, novel pharmacological strategies that inhibit TLR7 or IRAK4 might be applied to treat the inflammation and fibrosis of affected organs.

## Acknowledgments

We thank Takuma Shibata PhD, Yuji Motoi, PhD, and Kensuke Miyake, MD, PhD, from the Division of Innate Immunity, Department of Microbiology and Immunology, Institute of Medical Science, University of Tokyo for their technical support, and Melissa Crawford, PhD, and J. Ludovic Croxford, PhD, from Edanz Group (<https://jp.edanz.com/ac>) for editing a draft of this manuscript.

## Author Contributions

All authors were involved in drafting the article or revising it critically for important intellectual content, and all authors approved the final version to be published. Dr. Moriyama had full access to all of the data in the study and takes responsibility for the integrity of the data and the accuracy of the data analysis.

**Study conception and design.** Chinju, Moriyama, Nakamura.

**Acquisition of data.** Moriyama, Kakizoe-Ishiguro, Haque, Furusho, Sakamoto, Kai, Kibe, Ito-Ohta.

**Analysis and interpretation of data.** Chinju, Moriyama, Chen, Miyahara, Hatakeyama-Furukawa, Maehara, Nakamura.

## References

1. Hamano H, Kawa S, Horiuchi A, Unno H, Furuya N, Akamatsu T, et al. High serum IgG4 concentrations in patients with sclerosing pancreatitis. *N Engl J Med* 2001;344:732-8.
2. Umehara H, Okazaki K, Masaki Y, Kawano M, Yamamoto M, Saeki T, et al. A novel clinical entity, IgG4-related disease (IgG4RD): general concept and details. *Mod*

Rheumatol 2012;22:1-14.

3. Stone JH, Zen Y, Deshpande V. IgG4-related disease. *N Engl J Med* 2012;366:539-51.
4. Nirula A, Glaser SM, Kalled SL, Taylor FR. What is IgG4? A review of the biology of a unique immunoglobulin subtype. *Curr Opin Rheumatol* 2011;23:119-24.
5. Tanaka A, Moriyama M, Nakashima H, Miyake K, Hayashida JN, Maehara T, et al. Th2 and regulatory immune reactions contribute to IgG4 production and the initiation of Mikulicz disease. *Arthritis Rheum* 2012;64:254-63.
6. Maehara T, Moriyama M, Nakashima H, Miyake K, Hayashida JN, Tanaka A, et al. Interleukin-21 contributes to germinal centre formation and immunoglobulin G4 production in IgG4-related dacryoadenitis and sialoadenitis, so-called Mikulicz's disease. *Ann Rheum Dis* 2012;71:2011-19.
7. Maehara T, Mattoo H, Ohta M, Mahajan VS, Moriyama M, Yamauchi M, et al. Lesional CD4<sup>+</sup> IFN- $\gamma$ <sup>+</sup> cytotoxic T lymphocytes in IgG4-related dacryoadenitis and sialoadenitis. *Ann Rheum Dis* 2017;76:377-85.
8. Tsuboi H, Matsuo N, Iizuka M, Tsuzuki S, Kondo Y, Tanaka A, et al. Analysis of IgG4 class switch-related molecules in IgG4-related disease. *Arthritis Res Ther* 2012;14:R171.
9. Zen Y, Fujii T, Harada K, Kawano M, Yamada K, Takahira M, et al. Th2 and regulatory immune reactions are increased in immunoglobulin G4-related sclerosing pancreatitis and cholangitis. *Hepatology* 2007;45:1538-46.
10. Moriyama M, Tanaka A, Maehara T, Furukawa S, Nakashima H, Nakamura S. T helper subsets in Sjögren's syndrome and IgG4-related dacryoadenitis and sialoadenitis: a



critical review. *J Autoimmun* 2014;51:81-8.

11. Akiyama M, Suzuki K, Yamaoka K, Yasuoka H, Takeshita M, Kaneko Y, et al. Number of circulating follicular helper 2 T cells correlates with IgG4 and interleukin-4 levels and plasmablast numbers in IgG4-related disease. *Arthritis Rheumatol* 2015;67:2476-81.
12. Mattoo H, Mahajan VS, Della-Torre E, Sekigami Y, Carruthers M, Wallace ZS, et al. De novo oligoclonal expansions of circulating plasmablasts in active and relapsing IgG4-related disease. *J Allergy Clin Immunol* 2014;134:679-87.
13. Nakamura T, Satoh-Nakamura T, Nakajima A, Kawanami T, Sakai T, Fujita Y, et al. Impaired expression of innate immunity-related genes in IgG4-related disease: A possible mechanism in the pathogenesis of IgG4-RD. *Mod Rheumatol* 2020;30:551-7.
14. Uchida K, Okazaki K. Clinical and pathophysiological aspects of type 1 autoimmune pancreatitis. *J Gastroenterol* 2018;53:475-83.
15. Nakajima A, Masaki Y, Nakamura T, Kawanami T, Ishigaki Y, Takegami T, et al. Decreased Expression of Innate Immunity-Related Genes in Peripheral Blood Mononuclear Cells from Patients with IgG4-Related Disease. *PLoS One* 2015;10:e0126582.
16. Furukawa S, Moriyama M, Tanaka A, Maehara T, Tsuboi H, Iizuka M, et al. Preferential M2 macrophages contribute to fibrosis in IgG4-related dacryoadenitis and sialoadenitis, so-called Mikulicz's disease. *Clin Immunol* 2015;156:9-18.
17. Furukawa S, Moriyama M, Miyake K, Nakashima H, Tanaka A, Maehara T, et al. Interleukin-33 produced by M2 macrophages and other immune cells contributes to Th2 immune reaction of IgG4-related disease. *Sci Rep* 2017;7:42413.

- Accepted Article
18. Yanagawa M, Uchida K, Ando Y, Tomiyama T, Yamaguchi T, Ikeura T, et al. Basophils activated via TLR signaling may contribute to pathophysiology of type 1 autoimmune pancreatitis. *J Gastroenterol* 2018;53:449-60.
  19. Yoshikawa T, Watanabe T, Minaga K, Kamata K, Kudo M. Cytokines produced by innate immune cells in IgG4-related disease. *Mod Rheumatol* 2019;29:219-25.
  20. Watanabe T, Yamashita K, Fujikawa S, Sakurai T, Kudo M, Shiokawa M, et al. Involvement of activation of toll-like receptors and nucleotide-binding oligomerization domain-like receptors in enhanced IgG4 responses in autoimmune pancreatitis. *Arthritis Rheumatol* 2012;64:914-24.
  21. Fukui Y, Uchida K, Sakaguchi Y, Fukui T, Nishio A, Shikata N, et al. Possible involvement of Toll-like receptor 7 in the development of type 1 autoimmune pancreatitis. *J Gastroenterol* 2015;50:435-44.
  22. Ishiguro N, Moriyama M, Furusho K, Furukawa S, Shibata T, Murakami Y, et al. Activated M2 Macrophages Contribute to the Pathogenesis of IgG4-Related Disease via Toll-like Receptor 7/Interleukin-33 Signaling. *Arthritis Rheumatol* 2020;72:166-78.
  23. Moriyama M, Furukawa S, Kawano S, Goto Y, Kiyoshima T, Tanaka A, et al. The diagnostic utility of biopsies from the submandibular and labial salivary glands in IgG4-related dacryoadenitis and sialoadenitis, so-called Mikulicz's disease. *Int J Oral Maxillofac Surg* 2014;43:1276-81.
  24. Umehara H, Okazaki K, Kawa S, Takahashi H, Goto H, Mastui S, et al. The 2020 revised comprehensive diagnostic (RCD) criteria for IgG4-RD. *Mod Rheumatol* 2021;31:529-33.
  25. Masaki Y, Sugai S, Umehara H. IgG4-related diseases including Mikulicz's disease and

- sclerosing pancreatitis: diagnostic insights. *J Rheumatol* 2010;37:1380-5.
26. Fujibayashi T, Sugai S, Miyasaka N, Hayashi Y, Tsubota K. Revised Japanese criteria for Sjögren's syndrome (1999): availability and validity. *Mod Rheumatol* 2004;14:425-34.
27. Shiboski CH, Shiboski SC, Seror R, Criswell LA, Labetoulle M, Lietman TM, et al, and the International Sjögren's Syndrome Criteria Working Group. 2016 American College of Rheumatology/ European League Against Rheumatism classification criteria for primary Sjögren's syndrome: a consensus and data-driven methodology involving three international patient cohorts. *Arthritis Rheumatol* 2017;69:35-45.
28. Ohta M, Moriyama M, Maehara T, Gion Y, Furukawa S, Tanaka A, et al. DNA microarray analysis of submandibular glands in IgG4-related disease indicates a role for MARCO and other innate immune-related proteins. *Medicine (Baltimore)* 2016;95:e2853.
29. Moriyama M, Hayashida JN, Toyoshima T, Ohyama Y, Shinozaki S, Tanaka A, et al. Cytokine/chemokine profiles contribute to understanding the pathogenesis and diagnosis of primary Sjögren's syndrome. *Clin Exp Immunol* 2012;169:17-26.
30. Fábio V M, Júlia S, Charles A, Marco T, Gabriela G, Gabrielle R, et al. Lack of IL-1 Receptor-Associated Kinase-4 Leads to Defective Th1 Cell Responses and Renders Mice Susceptible to Mycobacterial Infection. *J Immunol* 2016;197:1852-63.
31. Umehara H, Okazaki K, Kawa S, Takahashi H, Goto H, Matsui S, et al. The 2020 revised comprehensive diagnostic (RCD) criteria for IgG4-RD. *Mod Rheumatol* 2021;31:529-33
32. Yamashina M, Nishio A, Nakayama S, Okazaki T, Uchida K, Fukui T, et al. Comparative study on experimental autoimmune pancreatitis and its extrapancreatic involvement in mice. *Pancreas* 2012;41:1255-62.

- Accepted Article
33. Haruta I, Yanagisawa N, Kawamura S, Furukawa T, Shimizu K, Kato H, et al. A mouse model of autoimmune pancreatitis with salivary gland involvement triggered by innate immunity via persistent exposure to avirulent bacteria. *Lab Invest* 2010;90:1757-69.
  34. Watanabe T, Yamashita K, Arai Y, Minaga K, Kamata K, Nagai T, et al. Chronic Fibro-Inflammatory Responses in Autoimmune Pancreatitis Depend on IFN- $\alpha$  and IL-33 Produced by Plasmacytoid Dendritic Cells. *J Immunol* 2017;198:3886-96.
  35. Sica A, Mantovani A. Macrophage plasticity and polarization: in vivo veritas. *J Clin Invest* 2012;122:787-95.
  36. Alessandro V, Rama M, Hyejeong C, Andrew J, Jeffrey D, Debra L, et al. Characterization of Distinct Macrophage Subpopulations during Nitrogen Mustard-Induced Lung Injury and Fibrosis. *Am J Respir Cell Mol Biol* 2016;54:436-46.
  37. Ewald SE, Barton GM. Nucleic acid sensing Toll-like receptors in autoimmunity. *Curr Opin Immunol* 2011;23:3-9.
  38. Capucine P, Anne P, Marion B, Cheng-L, Jacinta B, Kun Y, Claire S, et al. Pyogenic bacterial infections in humans with IRAK-4 deficiency. *Science* 2003;299:2076-9.
  39. Suzuki N, Suzuki S, Duncan GS, Millar DG, Wada T, Mirtsos C, et al. Severe impairment of interleukin-1 and Toll-like receptor signalling in mice lacking IRAK-4. *Nature* 2002;416:750-6.
  40. Leah C, Aaron W, Scott A, Jelinsky, Katherine L, Wouter K, Rachael H, et al. IRAK4 kinase activity controls Toll-like receptor-induced inflammation through the transcription factor IRF5 in primary human monocytes. *J Biol Chem* 2017;292:18689-98.

## Figure Legends

**Figure 1.** TLR7-related gene expression patterns in salivary glands (SGs) from patients with IgG4-related disease (IgG4-RD) and *human TLR7*-transgenic/*mTlr7* deficient (Tg) mice. (A) Tg and *mTlr7*<sup>-/-</sup> (KO) mice at 4 weeks old after stimulation with the TLR7 agonist R848 (B) Hematoxylin and eosin (H&E) and Masson's trichrome (MT) stained sections of submandibular glands (SMGs) from representative Tg and KO mice. (C) Fibrosis scores of SMG or (D) serum IgG and IgG1 levels in Tg and KO mice (n = 6/sample). Heat map depicting differentially-expressed TLR7-related genes in SMGs from Tg and KO mice (E) or IgG4-RD patients and healthy controls (HCs) (F). Only genes upregulated or downregulated at least twofold are shown. mRNA expression levels of candidate TLR7-related genes in the SGs from Tg (n = 6) and KO (n = 6) mice (G) or HCs (n = 15) and patients with chronic sialadenitis (CS) (n = 10), Sjögren's syndrome (SS) (n = 15), and IgG4-RD (n = 15) (H). *N.S.* = not significant. Scale bars = 100  $\mu$ m. Bars show the mean  $\pm$  SD. \* =  $P < 0.05$ ; \*\* =  $P < 0.01$  by Mann-Whitney *U*-test (C, D, F) or Kruskal-Wallis test (H).

**Figure 2.** Identification and distribution of IRAK4 in SMGs from patients with IgG4-RD and Tg mice. Distribution of candidate TLR7-related molecules in SMGs from representative Tg and KO mice (A), HCs, and patients with CS, SS, and IgG4-RD (B), or normal tonsil, normal lymph node, and SMG from patients with IgG4-RD (C). Outlined area indicates a germinal center (GC). (D) Number of IRAK4-positive cells in SGs from HCs and patients with CS, SS, and IgG4-RD measured using TissueQuest software. (E) Each set of serial sections was stained with H&E, and antibodies to IRAK4, CD80, CD163, CD11c, and CD123. Scale bars = 100  $\mu$ m. (F) Double immunostaining for IRAK4 (red), CD80 (green), CD163 (green), CD11c (green), and CD123 (green) in SMGs from representative patients with IgG4-RD. Counterstaining was performed with DAPI (blue). Scale bars = 100  $\mu$ m. (G) Number of

IRAK4-expressing CD80-, CD163-, CD11c-, and CD123-positive cells in SMGs from patients with IgG4-RD (n = 12) measured using TissueQuest software. Bars show the mean  $\pm$  SD. \* =  $P < 0.05$ ; \*\* =  $P < 0.01$  by Kruskal–Wallis test (D, G). See Figure 1 for other definitions.

**Figure 3.** Expression of inflammatory cytokines and candidate TLR7-related genes in M2 macrophages. (A) Schematic illustration of the extraction of human CD163<sup>+</sup> M2 macrophages stimulated by the TLR7 agonist loxoribine and/or IRAK4 inhibitor CA-4948. (B) Detection of CD163 and TLR7 before/after the differentiation and selection of M2 macrophages (Day 0, Day 6) from at least two independent experiments, as determined by flow cytometric analysis. (C) Schematic representation of TLR7 pathways. (D) mRNA expression levels of TLR7-related genes in human CD163<sup>+</sup> M2 macrophages cultured in the presence or absence of loxoribine and CA-4948 (n = 6/sample). (E) The production of inflammatory cytokines in CD163<sup>+</sup> M2 macrophages stimulated with/without loxoribine and CA-4948, as determined by ELISAs. Bars show the mean  $\pm$  SD. \* =  $P < 0.05$ ; \*\* =  $P < 0.01$  by Mann–Whitney *U*-test (D) or Kruskal–Wallis test (E). IL-33 = interleukin-33, TGF- $\beta$  = transforming growth factor- $\beta$ . See Figure 1 for other definitions.

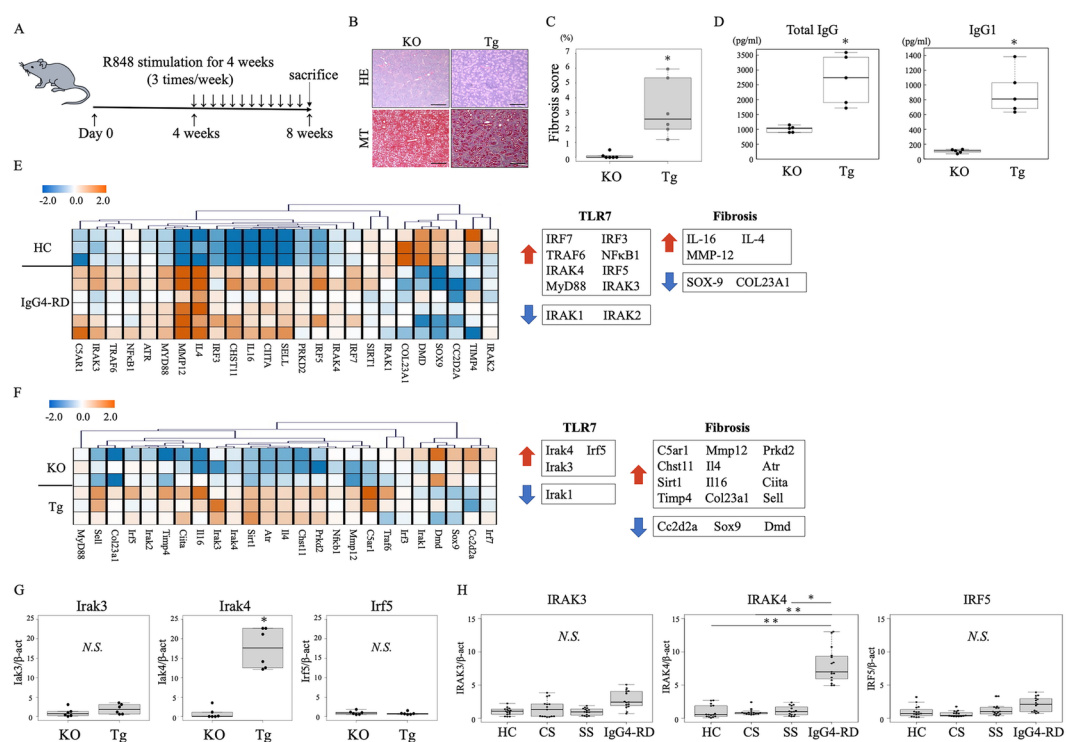
**Figure 4.** Involvement of M2 macrophages in the proliferation and activation of fibroblasts. (A) Schematic illustration of the co-cultivation of human fibroblasts (MRC-5 cells) with the conditional medium (CM) of CD163<sup>+</sup> M2 macrophages stimulated with loxoribine and/or CA-4948. (B) Representative image of MRC-5 cells cultured in the CM of CD163<sup>+</sup> cells with/without loxoribine and CA-4948. Scale bars = 100  $\mu$ m. (C) Proliferation of MRC-5 cells cultured in the CM of CD163<sup>+</sup> cells with/without loxoribine and CA-4948 (n = 6/sample). (D) mRNA expression levels of fibrosis-related genes in MRC-5 cells with/without loxoribine and CA-4948 (n = 6/sample). (E) The production of type 1 collagen in MRC-5 cells stimulated

with/without loxoribine and CA-4948, as determined by ELISAs. Bars show the mean  $\pm$  SD.

\* =  $P < 0.05$ ; \*\* =  $P < 0.01$  by Kruskal–Wallis test. See Figure 1 for other definitions.

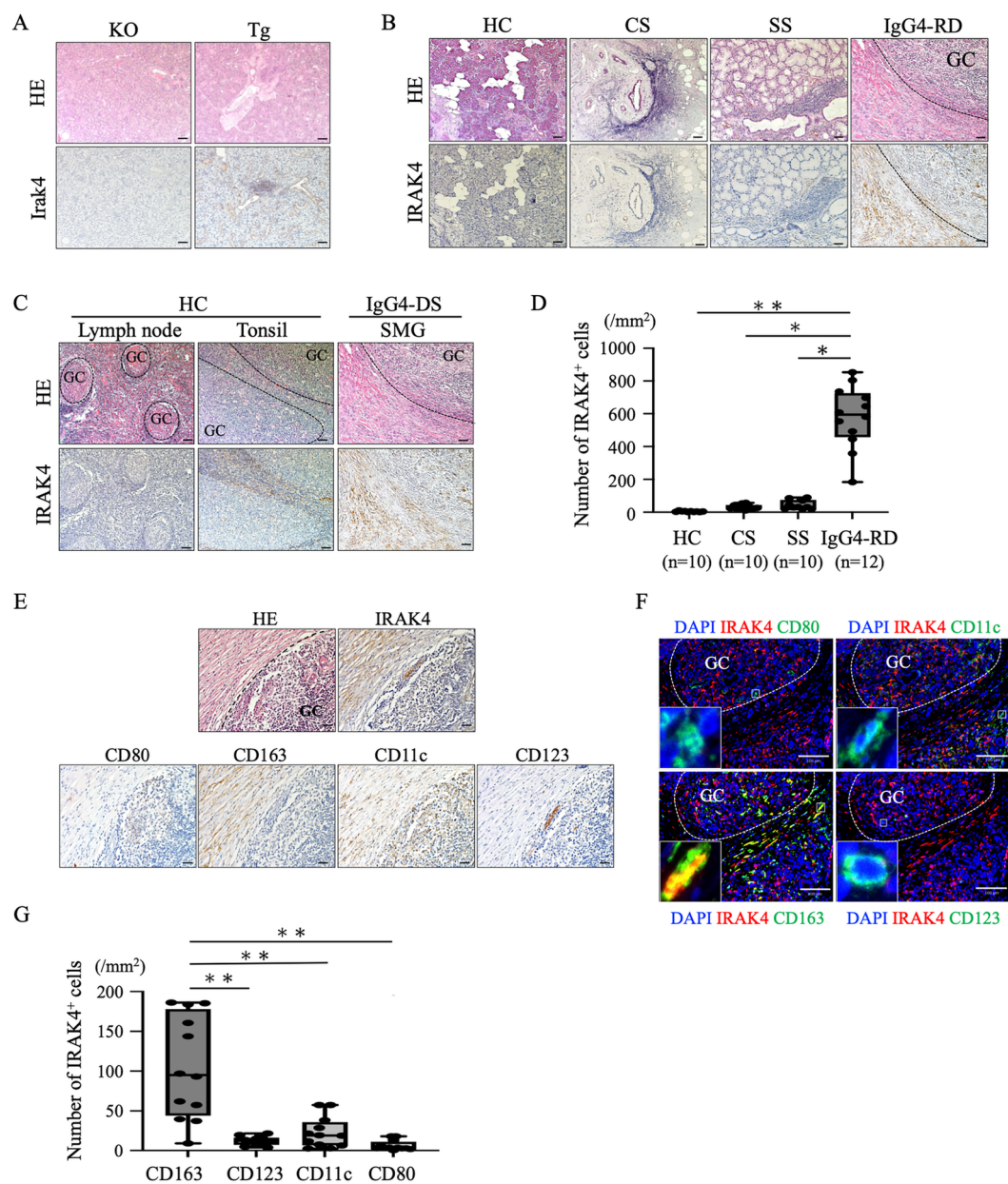
**Figure 5.** Correlation between fibrosis and M2 macrophages in SMGs from patients with IgG4-RD. (A) Each set of serial sections was stained with H&E, MT, or antibodies to CD163, and IRAK4. Scale bars = 100  $\mu$ m. (B) Correlation between the fibrosis score and number of CD163- or IRAK4-positive cells in SMGs (n = 12/sample). Number of CD163- and IRAK4-positive cells was measured using TissueQuest software. MT staining was performed as described in the Patients and Methods section. The correlation coefficients and  $P$ -values were determined using Spearman's rank correlation. See Figure 1 for other definitions.

**Figure 6.** Schematic model of TLR7 signaling in M2 macrophages leading to fibrosis in IgG4-RD. TLR7 expressed on M2 macrophages recognizes some viral RNAs or self RNAs released from stressed or injured cells. Activated M2 macrophages secrete fibrotic cytokines, including IL-1 $\beta$ , TGF $\beta$ , and IL-33, via IRAK4/NF- $\kappa$ B signaling, which leads to fibrosis. See Figure 1 for other definitions.

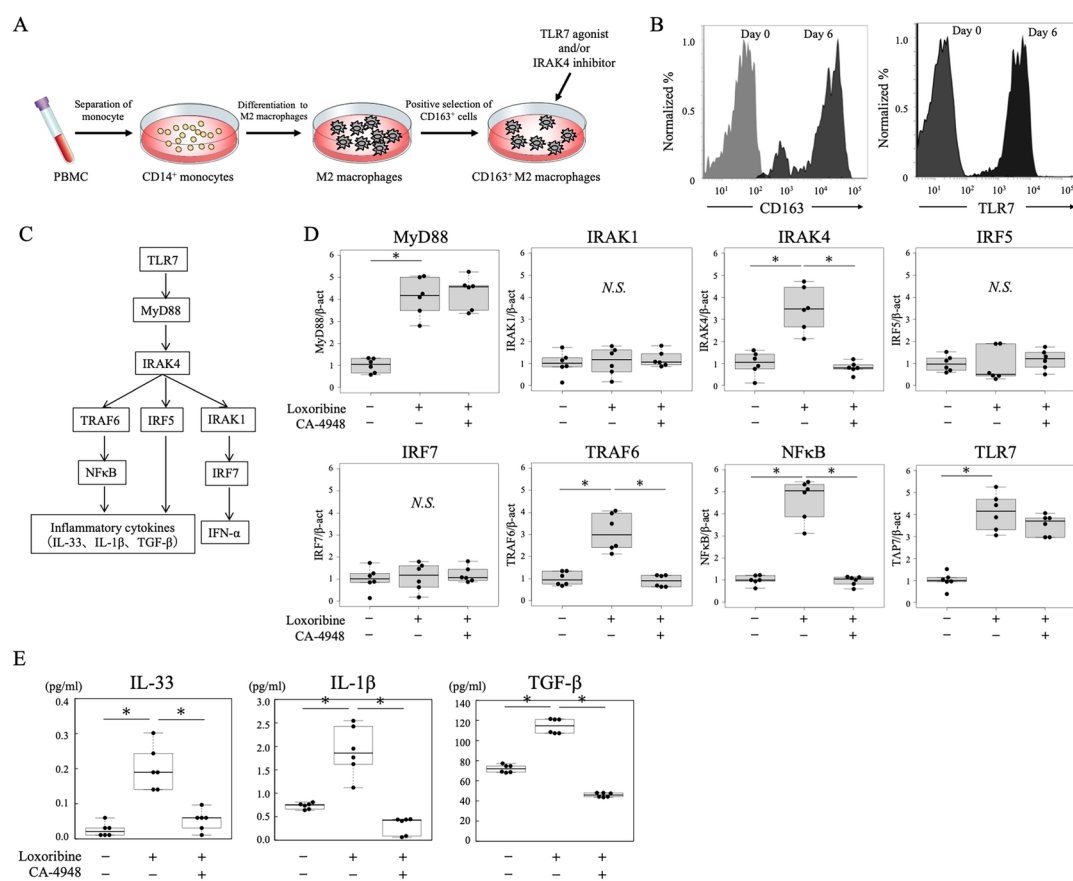


ART\_42043\_Figure 1 (350dpi)-7.tif

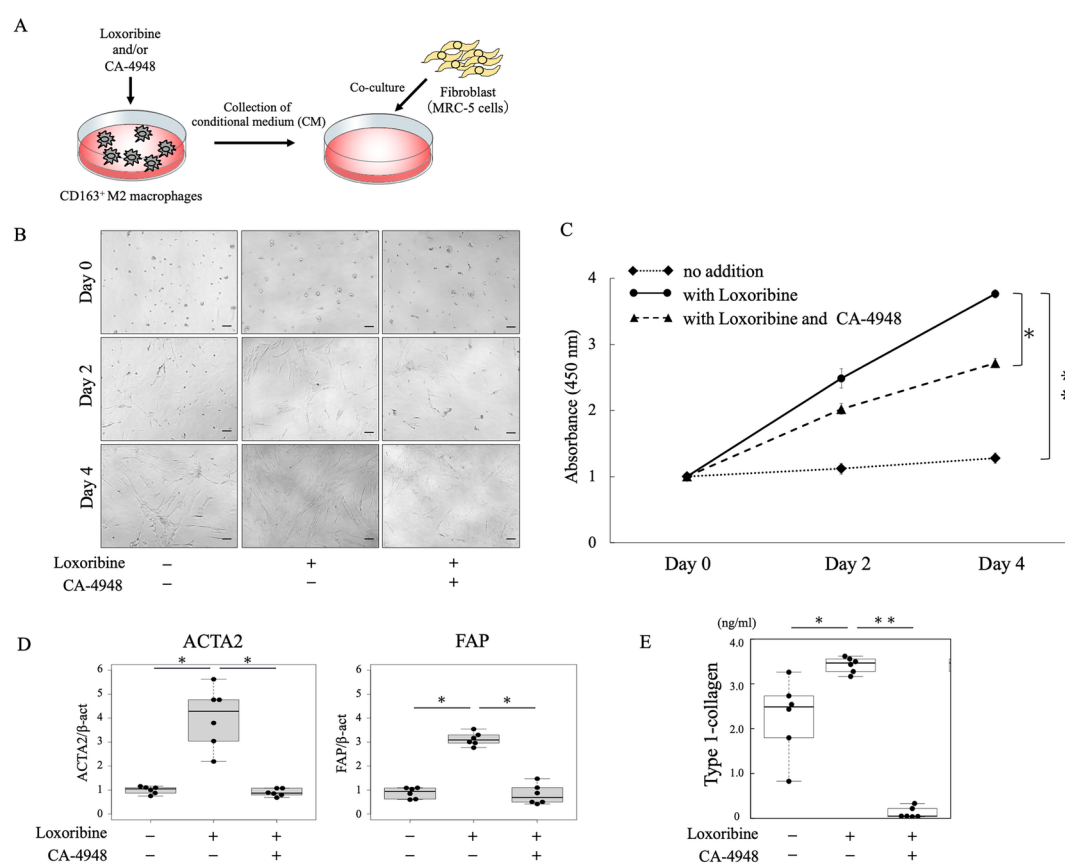




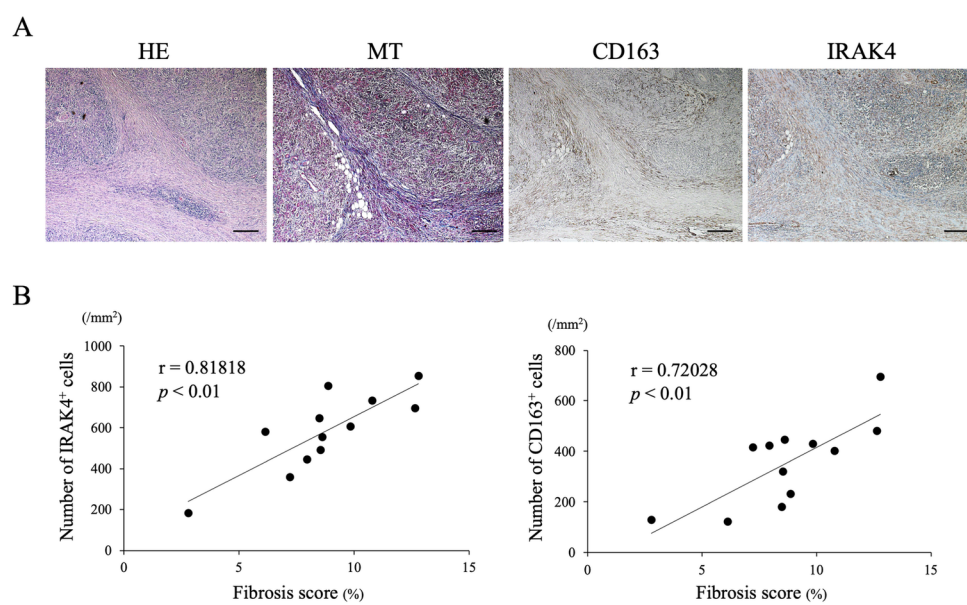
ART\_42043\_Figure 2 (350dpi)-2 .tif



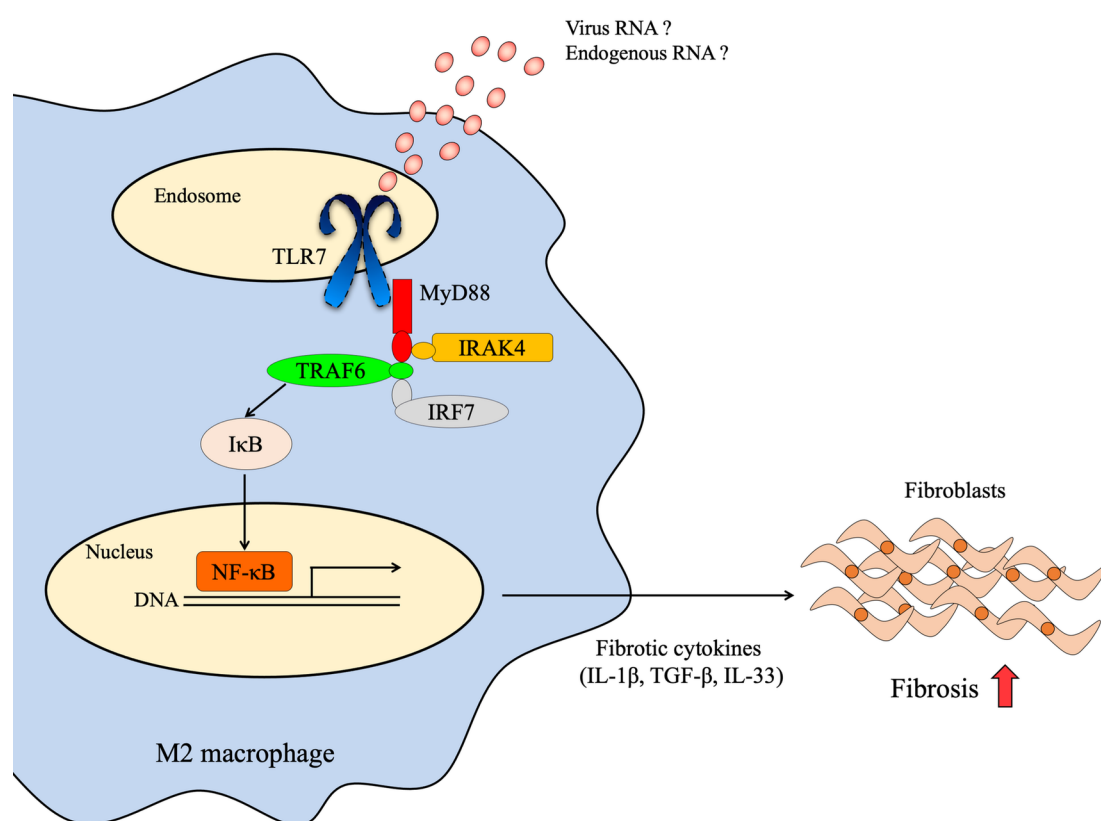
ART\_42043\_Figure 3 (350dpi)-2 .tif



ART\_42043\_Figure 4 (350dpi)-2 .tif



ART\_42043\_Figure 5 (350dpi).tif



ART\_42043\_Figure 6 (350dpi).tif